

Commissioning of NASA's 3rd Generation Tracking and Data Relay Satellites (TDRS KLM)

Jennifer Donaldson¹, Gregory Heckler², Cheryl Gramling³, Benjamin Ashman⁴, Marco Toral⁵, and Christopher Carson⁶

NASA Goddard Space Flight Center, Greenbelt, MD, 20771, USA

and

Jeremy Lyon⁷

Boeing Intelligence and Analytics, Annapolis Junction, MD, 20701, USA

In the summer of 2017, the third and final spacecraft of the 3rd generation of the Tracking and Data Relay Satellites (TDRS) launched aboard an Atlas V rocket from Complex 41 on the Eastern Test Range. Finishing final testing and integration in the first quarter of 2018, the TDRS-M communication and navigation satellite completes a constellation that began service in the early 1980s. The 3rd generation of spacecraft, TDRS-K, L, and M, not only provided beneficial systems engineering lessons in handling anomalous Radio Frequency and Doppler interference as well as integrating new spacecraft into an aging ground support infrastructure, but also supplies NASA with a valuable test bed for new operational concepts and technologies useful in defining the future architecture of the NASA Space Network. This paper presents an overview of the TDRS-K, L, and M missions, including transfer orbit, Level 5 bus and payload testing, and finally NASA-led Level 6 testing, which includes active TDRS System (TDRSS) users. Highlights include relevant testing results, commissioning challenges, and lessons learned. The final discussion includes a brief overview of future NASA communication and navigation technologies and network architectures.

I. Introduction

The National Aeronautics and Space Administration's (NASA) Tracking and Data Relay Satellite (TDRS) System (TDRSS), also known as the Space Network (SN), consists of a fleet of ten inclined geosynchronous satellites longitudinally spaced in three oceanic regions: Atlantic, Pacific, and Indian. Ground stations are located at Las Cruces, New Mexico, Guam, and Blossom Point, Maryland, as viewed in Figure 1. The ground system provides the time and frequency reference, signal processing, data modulation for command and demodulation for telemetry of both the TDRS and the user service signals, as well as range and Doppler radiometric observations. The SN supports a wide array of customers, notably Human Space Flight International Space Station and cargo resupply missions, launch vehicles, the suite of Earth Observing System missions, Space Science missions that study astrophysics, heliophysics, and the cosmos, and outposts on Earth for science ventures. Coverage for these missions, referred to as User Satellites or USATs, range from launch pad to low earth orbit to highly elliptical orbits, with the SN providing command, telemetry, and radiometric tracking services in three frequency bands (S-, Ku-, and Ka-band). The capacity for each of the recent six TDRS includes: two forward and five return services via the Multiple Access (MA) S-band phased array, one forward and one return service from each of two 4.6-meter parabolic gimbaled Single Access (SA) tri-feed antennas at both S-band and K-band. Only one USAT can utilize the SA antennas at a time, but can receive multiple services simultaneously, if desired. Figure 2 depicts the 3rd generation TDRS spacecraft in the deployed configuration.

¹ TDRS-M Payload Test Engineer, Navigation and Mission Design Branch, NASA GSFC, AIAA Member

² Deputy Telecommunications Systems Manager, Tracking Data Relay Satellite Project, NASA GSFC, AIAA Member

³ TDRS-M Mission Segment Manager, Navigation and Mission Design Branch, NASA GSFC, AIAA Senior Member

⁴ TDRS-M Flight Dynamics Lead, Navigation and Mission Design Branch, NASA GSFC

⁵ Telecommunications Systems Manager, Tracking Data Relay Satellite Project, NASA GSFC

⁶ Flight Integration Manager, Tracking Data Relay Satellite Project, NASA White Sands Complex NM

⁷ TDRS-M Flight Operations Lead – TDRS Analyst, SCNS Spacecraft Operations Engineering, NASA White Sands Complex NM

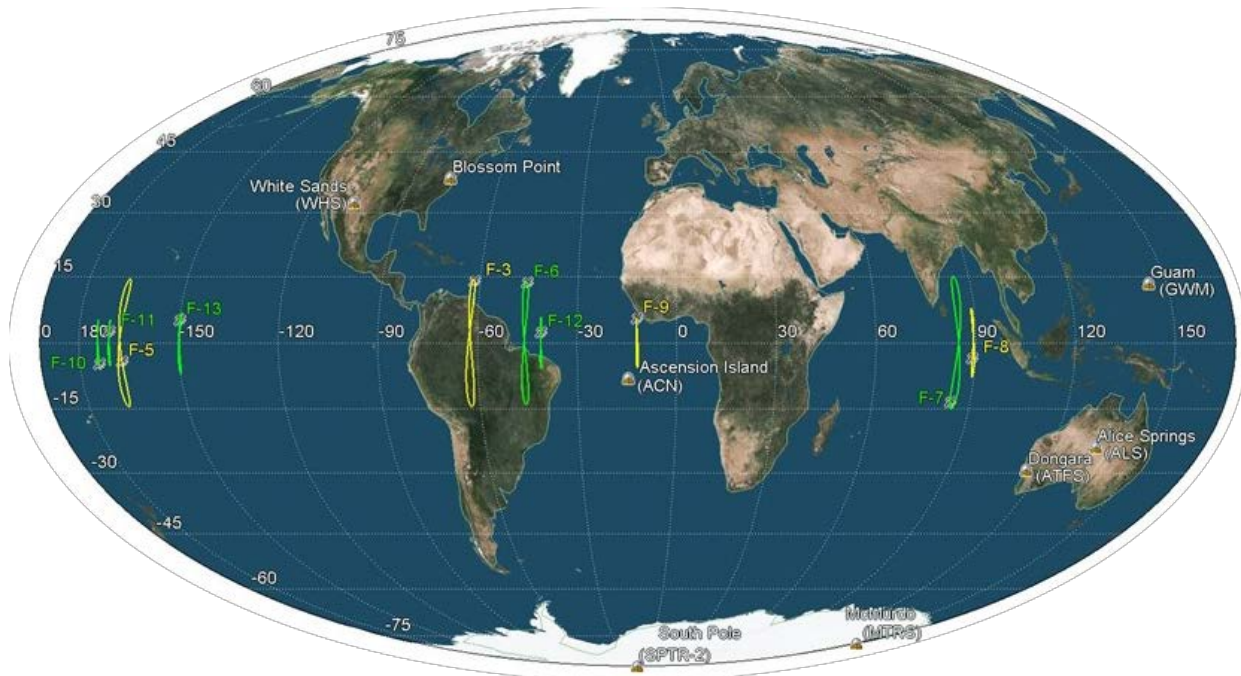


Figure 1. Global View of the Space Network Elements

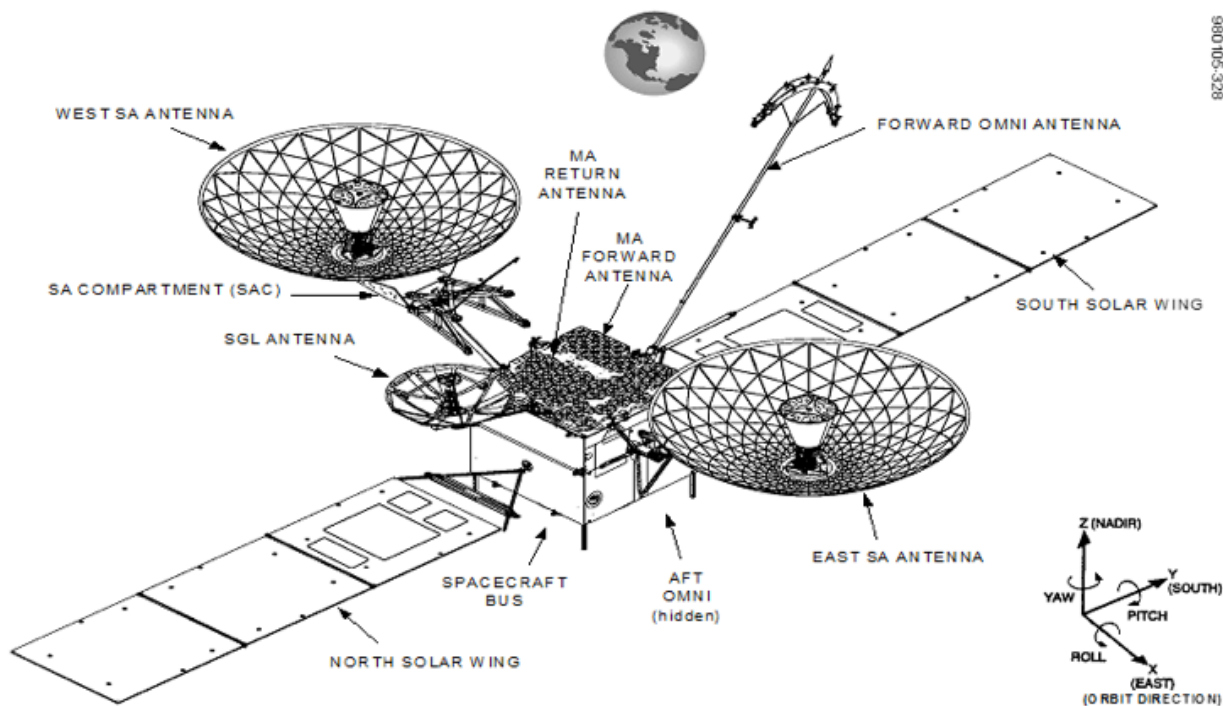


Figure 2. Third Generation Tracking and Data Relay Satellite Overview

The three newest TDRS to join the fleet were built and delivered to orbit under contract with The Boeing Company (Boeing) in El Segundo, CA. The deliverables included modifications to the hardware, software, and test and simulation systems of the White Sands Complex (WSC) controlling ground segment based on requirement updates for the 3rd generation TDRS KLM spacecraft (S/C). After launch, each of the 3rd generation TDRS executed a transfer orbit and comprehensive On Orbit Testing (OOT) to verify expected performance. After acceptance, the S/C name

transitioned to an operational fleet craft number listed in Table 1. As the last of the 3rd generation spacecraft and relays of this configuration, TDRS KLM enables the Space Network’s ability to serve the user mission set well into the next decade as the next generation system matures.

Table 1. Third Generation TDRS Milestones

TDRS LAUNCH NAME	LAUNCH DATE	ACCEPTANCE DATE	OPERATIONS NAME
TDRS-K	January 30, 2013	August 16, 2013	TDRS-11
TDRS-L	January 24, 2014	June 27, 2014	TDRS-12
TDRS-M	August 18, 2017	February 8, 2018	TDRS-13

II. The Third Generation TDRS Spacecraft

The TDRS KLM spacecraft are built upon the Boeing 601 bus and operate at the geosynchronous altitude in the Earth centered, three-axis stable configuration. The 2.5-meter cube bus hosts all components needed for operations. At launch, the spacecraft has a mass of 3500 kg; the fully deployed span of TDRS is 13.6 x 21 meters. The S/C design provides service for 11 years in geosynchronous Earth orbit and four additional years of on-orbit storage. TDRS KLM are functionally identical to their TDRS HIJ predecessors, with the most significant difference in the relocation of the Multiple Access Return (MAR) beamformer to the ground. The bus is equipped with two sun tracking solar arrays producing 3.5 kW and a 123 Amp hour battery to provide the electrical power needs. Bus voltage remains-regulated at a constant level and autonomously provides seamless transitions between sunlight and eclipse periods. Thermal environmental control occurs autonomously via thermostatically controlled heaters, insulation blankets, heat pipes, radiator panels, and plume shields.

Tracking, Telemetry and Command (TT&C) is maintained primarily at Ku-band when the payload is configured for service mode, via a gimballed 1.8-meter parabolic Space to Ground Link (SGL) antenna. Two omni-directional S-band antennas (one nadir and one zenith) are used following launch through orbit raising and bus testing, and for storage and contingency operations. System redundancy and cross-over capabilities allow for dual S- and Ku-band operations, if needed. A dual Ku-band frequency plans allow for collocation with another TDRS. The phase modulated telemetry and command links operate as vertically polarized at Ku-band and Right Hand Circularly Polarized at S-band. Tone ranging provides the means for radiometric tracking.

Orbit insertion, maintenance, and attitude control are managed by a bipropellant liquid propulsion system which consists of two monomethylhydrazine (fuel) tanks, two nitrogen tetroxide (oxidizer) tanks, two helium (pressurant) tanks, twelve 10 N thrusters and a 490 N liquid apogee motor (LAM). The propulsion system is pressure-regulated during orbit insertion, and in blowdown once on station. The 490 N motor is only used during orbit insertion and disabled once the spacecraft is on station. Eight of the twelve 10 N thrusters are located near the corners of the north and zenith faces of the bus for attitude control, with two of the other four on each of the east and west faces near the center of mass for radial, in-track, and cross-track orbit maintenance.

Bus and antenna pointing is managed by the on-board Attitude Control Subsystem (ACS), which consists of sensors, actuators, and processors. Data from inertial reference units and earth and sun sensors are processed along with the spacecraft ephemeris to determine attitude errors. These errors are corrected by a two-axis gimballed momentum wheel and/or thrusters, depending on the control mode. Attitude errors are also forwarded to the SA gimbals to ensure pointing accuracy. Strategic solar array offsets are applied cyclically to negate roll/yaw momentum buildup. Thruster control is required periodically for pitch momentum maintenance. Every component of the ACS is fully redundant and monitored by onboard fault protection. Fault protection is configured to monitor for component or system level issues and autonomously respond to ensure spacecraft safety. Figure 3 shows a top level block diagram of the interaction between the different subsystems, such as the Electrical Power, Propulsion, TT&C, Payload, and ACS.

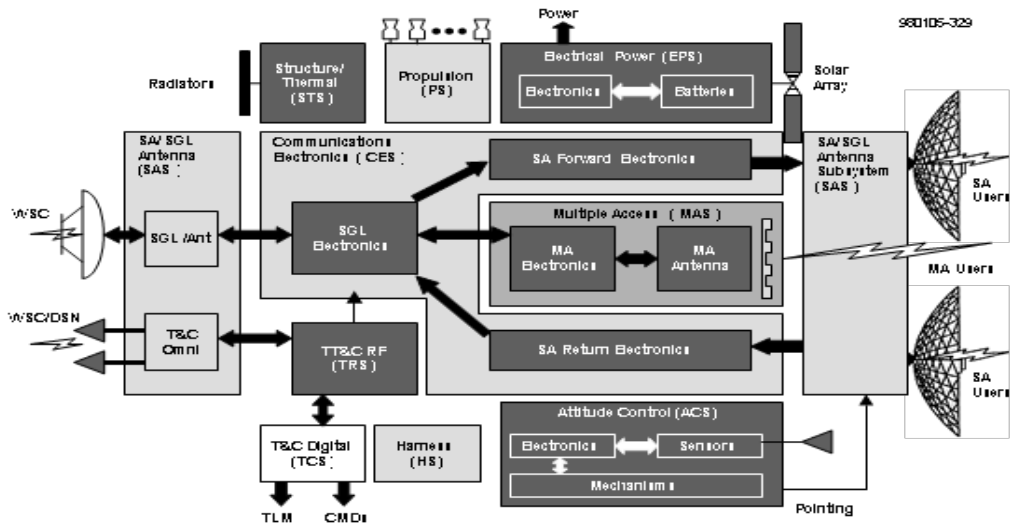


Figure 3. Satellite Block Diagram

The SA programmed pointing mode, known as Program Track, is the primary method for steering the single access antennas within their Field of View (FOV) of 75.7 deg of azimuth in the outboard direction, 23.0 deg in the inboard direction, and +/- 29.4 deg in elevation. The S-band and Ka-band SA services are tunable, while S-band MA and Ku-band SA services operate on fixed frequencies. The spacecraft forward channel bandwidths range from 6 MHz to 50 MHz and return channel bandwidths range from 6 MHz to 650 MHz. The satellites support two 225-MHz wide Ku-band or Ka-band SA return channels, and can be configured to make one 650-MHz wide Ka-band return channel. The SA reflector can be switched between Right Hand Circular and Left Hand Circular polarizations. For receiving return signals, the Ku- and Ka-band antenna feeds include a provision for a closed loop pointing mode called autotrack. The autotrack system consists of an onboard RF system to sense the antenna pointing errors and command generation equipment on the ground to close the loop. This is particularly important at Ka-band where the narrow antenna beamwidth requires accurate pointing to meet expected link performance.

TDRS KLM MA services are provided through a 47-element phased array antenna. This 47-element array is comprised of 15 transmit-only elements, 12 of which are used nominally for forward service, and 32 receive-only elements, 30 of which are used nominally for return service. A total of two forward beams can be formed by the on-board beamformer and six return beams can be formed by the ground-based beamformer. The FOV of the formed beam is ±13 deg from the center of the Earth; this FOV supports low Earth orbiting satellites from the TDRS geosynchronous orbit.

III. Description of TDRS Commissioning Activities

On Orbit Testing for TDRS KLM focuses on Bus OOT (BOOT) and Payload OOT (POOT) to verify that the launch environment introduced no issues or performance degradation to the spacecraft, and to validate all end to end services through the updated ground segment at WSC and TDRS to the USATs. The joint contractor and government Mission Operations team conducts OOT in three phases: Level 5A verifies the spacecraft, Level 5B verifies the spacecraft compatibility with the ground, and Level 6 validates the end-to-end services provided by the SN via the new relay spacecraft. Figure 4 provides a time-overview of the on orbit testing phases.

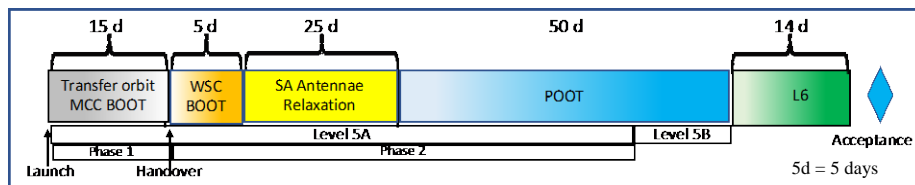


Figure 4. Time-based Overview of On Orbit Testing

Prior to the launch of TDRS-K, the team developed a comprehensive set of Test Procedures that identify test objectives, methodology, test set-up and equipment, detailed step-by-step instructions, data recording and artifact identification, and accept/reject criteria. The procedures include use of existing and new Local Operating Procedures (LOPs) developed for WSC operation of the 3rd generation spacecraft. Each phase of testing follows a pre-ordained Sequence of Events (SOE), which incorporates flexibility to rearrange testing as circumstances dictate.

A. Launch and Orbit Raising

Level 5A testing begins at the Boeing Mission Control Center during the 11-day transfer orbit, performing the bus functionals and spacecraft health checkouts of each subsystem. These checkouts occur while raising perigee and lowering inclination over five LAM maneuvers to deliver the spacecraft to its 7-deg inclined geosynchronous on-station test location at 149.8 deg West longitude. Deployments of the SA antennas, solar arrays, omni and parabolic SGL antennas followed the orbit raising, ending with the spacecraft in the ACS Normal mode, prepared to handover command control to WSC.

B. Level 5 Test Campaign

The BOOT portion of Level 5A continues from WSC for five days. Testing is conducted by a Flight Director and executed via a Satellite Controller familiar with the SN command and telemetry systems, WSC operating environment, and the LOPs. POOT commences after a 45-day SA relaxation period following the unfurlment of the SA antennas, with full payload power-on and configuration. POOT begins on the redundant side components with SGL calibration, then follows the SOE to perform calibrations and take pattern measurements of each user service antenna. Precise calibration tasks include antenna shape measurement and adjustment via a tuning mechanism at the base of the hub, boresighting, pseudorandom noise code and autotrack phase alignment for the SAs, and antenna pointing. Characterization of each service includes comparison to factory predictions of the OOT measurements of carrier to noise ratio (C/N_0), gain transfer for Effective Isotropic Radiated Power, frequency response, and frequency conversions to achieve established frequencies within each band. Once complete on the redundant side, the payload switches to the primary set of electronics for the team to repeat the service characterizations. Additional testing on the primary side focuses on examination of specific RF spurs, interference between the S-band service on the SAs, and the autotrack performance.

Once the spacecraft function and full performance verification completes in Level 5A, Level 5B testing then demonstrates compatibility between the ground segment at WSC and the spacecraft for all user services and modes. Measurements in Level 5B include Bit Error Counts, C/N_0 , and range and Doppler tracking service validity for coherent and non-coherent modes in both spread spectrum and non-spread spectrum data groups. POOT testing completes in approximately 53 days.

C. Level 6 Test Campaign

The prime objective for the last 14-day phase of OOT relies heavily on the operational USATs to verify interfaces and perform services from the user Mission Operations Centers through the SN to the TDRS under test to the user mission S/C, and through the return path. In addition, this Level 6 phase incorporates specialized tests to simulate nominal and stressing operational scenarios. These scenarios include the ACS ability to maintain high-rate, narrow beam user services under expected disturbances, measuring degradation of any service when the spacecraft executes fully loaded services, handovers of TDRS operations, performing navigation acceptance for radiometric tracking, acquisition vectors and antenna pointing for multiple scenarios, and operational thruster calibration. Following the 112 days of OOT, the TDRS spacecraft configuration switches to S-band storage mode until spacecraft acceptance.

IV. TDRS Challenges and Lessons Learned

As with any mission, throughout the course of pre-launch preparation and simulations, the mission operations team learns lessons to apply to the post-launch mission execution. With a series of spacecraft like TDRS, lessons learned during the execution of each spacecraft test campaign are carried over into improved execution for the successive spacecraft. For the three spacecraft in the TDRS KLM series, the team overcame several challenges resulting in significant lessons learned for not only TDRS, but for upcoming ground segment updates or missions with similar components or operations concepts. The following selection of specific lessons learned start with the spacecraft and branch out to the test environment.

A. Scalable Space Inertial Reference Unit (SSIRU) to Mechanical IRU for Launch and Orbit Raising

Throughout transfer orbit, the 3rd generation spacecraft is an unstable, minor axis spinner. Prior to the launch of TDRS-K, the baseline primary rate sensor for all phases of the TDRS-K mission was the Single 4-axis Scalable Space Inertial Reference Unit (SSIRU) using the gyro axes A, B and C out of the four axes and a Single 3-axis Mechanical Inertial Reference Unit (MIRU) was the backup sensor.

To maintain stability and to orient the spacecraft as needed, nutation and attitude control is provided by the ACS. Three types of control are used for TDRS KLM: Gyro/Wheel Active Nutation Control (GWANC), Thruster Active Nutation Control (TANC), and Thruster Spin Control (TSC). TANC is a rate-only phase plane thruster control, which uses the roll rate estimate to damp nutation from large angle motion until the rate error is below the deadband threshold. GWANC provides nutation control on wheels, which keeps the spacecraft spinning about the S/C body Z-axis. TSC is a proportional thruster control, which uses propagated quaternion attitude estimates and SSIRU (or MIRU) rate information to provide three axis spacecraft attitude and rate control.

Following TDRS-K launch and separation, the SSIRU reported rate data that was not as expected. As presented in Figure 5, the SSIRU sensor noise represents the SSIRU body rate data sampled over 0.0328 seconds where there was a 0.125 Hz cycle underneath an approximately 9-minute “beat” frequency observed in roll and pitch. This ripple caused the momentum wheel torque to saturate upon enabling GWANC control. The observed SSIRU rates were confirmed to not represent actual spacecraft dynamics by turning on the backup MIRU sensor for an independent assessment of the spacecraft rates.

Although the SSIRU had a significant flight history, TDRS-K stood as the first program to use a SSIRU in Whole Angle Mode (WAM) due to higher transfer orbit spin rate (5 RPM). In WAM, the gyro vibrational nodes move around the wine-glass shaped resonator, with the nodal rate of motion proportional to the SSIRU body rate. Hence, the 0.125 Hz oscillation seen in the SSIRU rate estimates in orbit represents a natural signature of WAM.

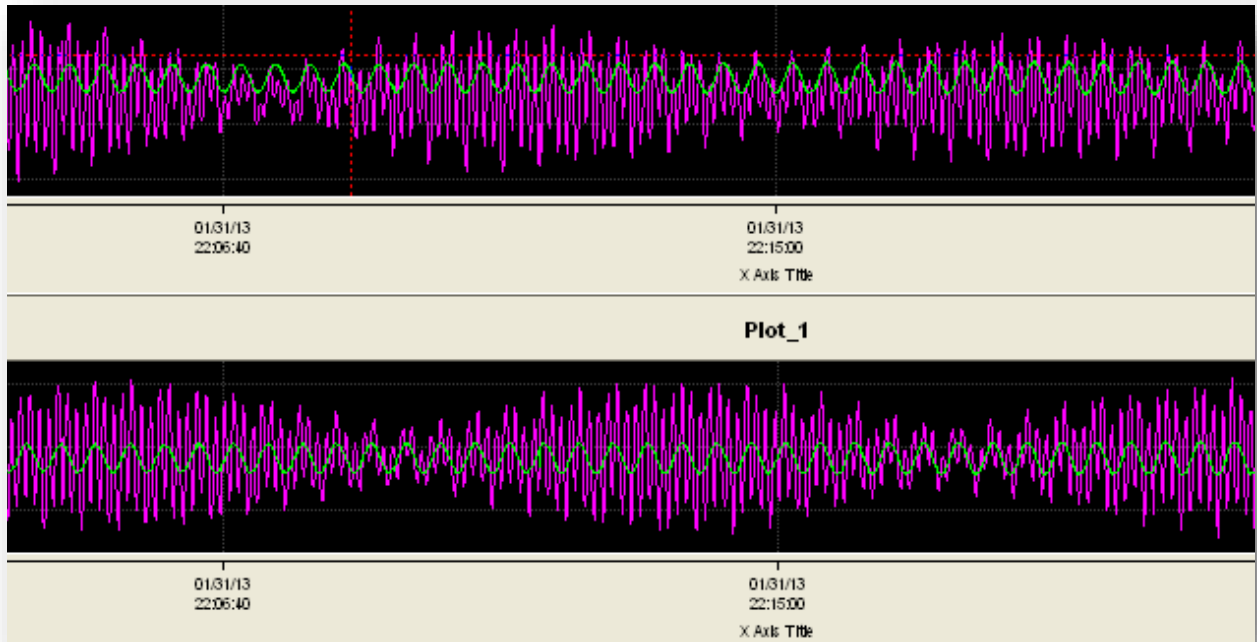


Figure 5. SSIRU (Magenta) and MIRU (Green) Overlaid Roll and Pitch Rates¹⁰⁰

Given the analysis, and to mitigate excess stress on the momentum wheel, the mission team redesigned the remainder of the transfer orbit to utilize the MIRU as the primary rate sensor. Following spin-down to deployments, the SSIRU performance returned to nominal and was re-selected as the primary rate sensor for the remainder of spacecraft life. For both subsequent TDRS, the baseline transfer orbit design was modified to use the MIRU for primary control with the SSIRU as backup.

B. Deployment Attitude Changes from TDRS-K, L and M

The mission deployment phase on TDRS KL commenced following completion of the last orbit raising apogee maneuver putting TDRS in geosynchronous earth orbit. Prior to deployments, a closed-loop attitude reorientation was performed to place the S/C in a sun normal attitude, adjusting the S/C Z-axis spin rate from 5.0 rpm to approximately 0.29 rpm and configuring the S/C actuators for deployment of the Solar Wings and Single Access Antennas. The baseline deployment sequence previously executed on TDRS-K started with a S/C reorientation to a 65 degree sun polar angle (SPA) for deployment of the north solar wing. After the north wing deployment, the S/C reorients to 45 deg SPA to maintain positive power, the momentum wheels were reconfigured, and the east and west SA booms deployed. The S/C was then reoriented to a 65 deg SPA, allowed to sit for 1.5 hours so that deployment mechanisms could reach acceptable temperatures, and then the south wing was deployed.

On TDRS-L, during the planned post-north wing deployment closed loop reorientation from 65 deg SPA to 45 deg SPA, a thruster limit cycle arose (Figure 6). The thruster-based reorientation maneuver was aborted and subsequent deployment of East & West Single Access Antennas and south solar wing were performed nominally at the current (aborted) attitude of 55 deg SPA.

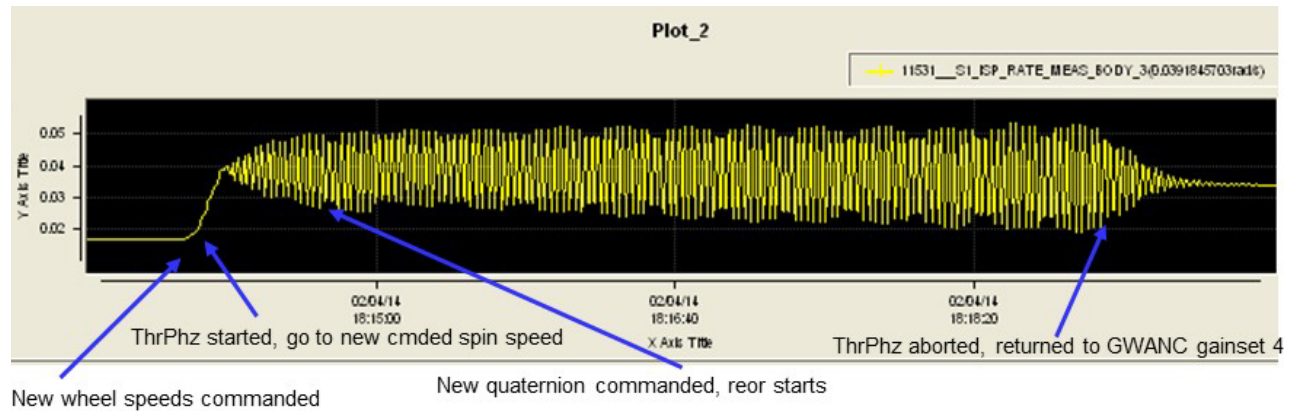


Figure 6. TDRS-L Flight Data: Raw Yaw Rate during Post N. Wing Deployment Reorientation¹⁰

The observed limit cycling during the deployment phase was determined to be due to an in-plane north wing flex mode not observed on the previous generation of TDRS or at the same amplitude on as on TDRS-K (Figure 7). Similar flex mode dynamics were observed during the post fully deployed reorientation on TDRS-K. A lesson learned action resulted in a controller update to mitigate deployed solar wing and thruster interaction in order to address this specific signature. TDRS-L and M post-deployments verified this successful update. The limit cycling event observed on TDRS-L during the reorientation maneuver in which only the north solar array was deployed was the result of north thruster interactions at about a 90% duty cycle resulting in an oscillation frequency near the in-plane flex dynamics.

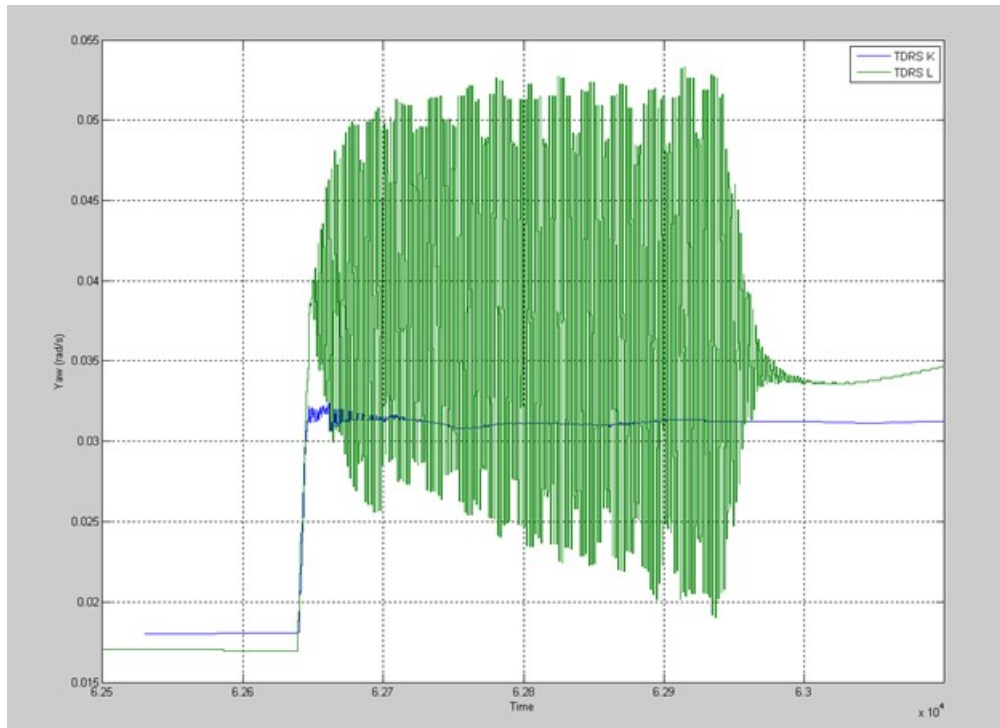


Figure 7. TDRS-K vs TDRS-L Yaw Rate comparison during Post N. Wing Deployment Reorientation¹⁰

For TDRS-M, the mission team assessed the robustness of the as-executed TDRS-L deployment sequence while maintaining a constant sun angle. The analysis concluded power and thermal deployment requirements for nominal and off nominal, non-steady state conditions and for an eclipse season deployment were satisfied and the ability to maintain telemetry and command links throughout the deployment sequence was re-verified. TDRS-M executed the new deployment sequence, updated from TDRS-L lessons learned, and all appendages were deployed nominally with no loss of telemetry or command capability while maintaining a positive power profile throughout the sequence.

C. Control System Gain Changes Due to Fuel Slosh

TDRS HIJ accomplished thruster flushing via momentum unloads independently of stationkeeping, which created operational inefficiencies. However, the auto-stationkeeping function of the TDRS KLM ACS allows for multiple maneuvers within the same maneuver window, providing a means for operations efficiency. The TDRS KLM project proposed streamlining the flushing process by utilizing this multi-maneuver capability, and designed the operational products required to do so. The pre-launch analysis of the combined stationkeeping and flushing maneuver was based on the TDRS HIJ analysis, which did not include fuel slosh as it was a minor effect. The combined maneuver was added to the routine maintenance regimen for TDRS KLM based upon TDRS HIJ flight performance lessons learned and analysis.

During OOT verification of the combined stationkeeping/thruster flushing maneuver, TDRS-K and TDRS-L experienced an attitude fault, which was ultimately attributed to propellant motion, also known as fuel slosh. After the first OOT fault was experienced, the simulation environment was reconfigured to incorporate a higher fidelity fuel particle model where simulations were compared against flight data which confirmed that the additional fuel loading made the fuel slosh a significant factor. The analysis concluded that the control system would benefit from updating the Pulsewidth Frequency Modulation (PFM) gains, adjusting the use of the proportional acceleration commands by increasing the bounding limits, and adjusting the input to the onboard auto-stationkeeping function itself.

The PFM function allows for residual computations of thruster torque requests to be carried from one computational cycle to the next. The initial PFM gains were set to 0 which discarded the torque request remainders, essentially creating an underperformance of the attitude control algorithm. The gain was updated to a value of 1, allowing for higher precision of torque requests to the control law. The bounding limit update consisted of zeroing out the acceleration estimates at the onset of the flushing activity and increasing the control limits to match flight

performance. It was determined that residual estimates from previous activities could corrupt the controller with the highly dynamic combined maneuvers which was not an issue with the more stable individual maneuvers.

The auto-stationkeeping update changed the gain state for the flushing portion of the maneuver to allow for higher acceleration estimates upon flushing completion. The fuel slosh created acceleration estimate fluctuations within the controller which were not sufficiently dampened upon transition to the attitude hold phase of the maneuver, resulting in insufficient momentum wheel torque command requests. The gain index was updated to use the high bandwidth value, allowing for proper control for the high dynamic transition. The implementation of these changes and improvements resulted in a reduction of attitude error from greater than 0.3 deg to less than 0.1 deg during combined flushing/stationkeeping maneuvers.

D. Maneuver Management Tool

USATs require accurate TDRS ephemeris predictions in order to produce their own real-time orbit knowledge provided as ancillary science data. These predicted orbit estimates must incorporate planned TDRS maneuvers. Errors between maneuver plans in the predicts and actual maneuver execution contributes to the uncertainty in USAT orbit knowledge and introduces additional operational efforts to improve the orbit knowledge in order to meet science requirements.

WSC and the Flight Dynamics Facility (FDF) discovered during TDRS-K that the provided propulsion model inaccurately represented the 10 N thrusters and the calibration lacked feedback tuning. The project sought a workaround to enable accurate maneuver planning for the 3rd generation S/C. In parallel to the development and commissioning of TDRS KLM, an update to modernize the Space Network ground segment is underway, as described in the following section on the Space Network Ground Segment Sustainment (SGSS). The updates include an enhancement to the SN TDRS maneuver planning, post-maneuver reconstruction, and calibration functions through creation of a Maneuver Management Tool (MMT). TDRS project and the SN took advantage of the SGSS effort to provide an early implementation of MMT at WSC for TDRS KLM that also incorporates improved propulsion models developed by the FDF for 3rd generation TDRS. The WSC implementation maintains compatibility with both the existing SN ground system and the ground system following SGSS deployment. MMT allows WSC to calibrate propulsion models using the post-maneuver Orbit Determination from FDF, thereby improving delta-v predictions and maneuver planning. The early integration and testing took place during the intervening period after TDRS-L acceptance and the launch of TDRS-M in order to leverage project tools, personnel, and activities, while simultaneously reducing risk for SGSS. The calibration process began during TDRS-M Level 6 testing, with plans to include all 3rd generation TDRS maneuvers to date. Testing performed during TDRS-M commissioning contributed significantly to identifying and resolving software scripting issues, paving the way for accurate TDRS maneuver and ephemeris predictions.

E. Radio Frequency Interference (RFI)

The SN's primary WSC ground station hosts five active space-to-ground-link terminals (SGLTs) as well as end-to-end test antennas (EETs). The S-, Ku-, and Ka-band EETs simulate SN user terminals. The EETs are used for monitoring TDRS payload performance over the life of the spacecraft as well as testing new upgrades or equipment deployed to the SNs ground segment. The EETs served as a critical resource to the Level 5 and Level 6 test campaigns; measurements taken with the EETs verify the health and performance of the TDRS payload after launch.

The WSC ground station also hosts three 19-meter S and Ka-band aperture antennas as part of NASA's Near Earth Network (NEN). These systems were installed in the mid 2000s to support the Solar Dynamics Observatory (SDO) and Lunar Reconnaissance Orbiter (LRO) missions.¹ As the SDO and LRO missions continued past their original mission lifetime, the NEN made the 19-meter apertures available to other users for scheduling S and Ka-band passes.

The co-location of the EET and NEN antennas created a near-far problem that beguiled the Level 5 and Level 6 test campaigns. The Ka-band EET is sufficiently distanced from the NEN antennas and no formal mitigation was necessary to deconflict NEN Ka-band downlinks with EET radiation. The S-band EET, however, is only 175 meters away from the SDO antenna and 280 meters from the LRO antenna. The distance and associated path loss did not provide sufficient isolation between the S-band EET and NEN antennas.

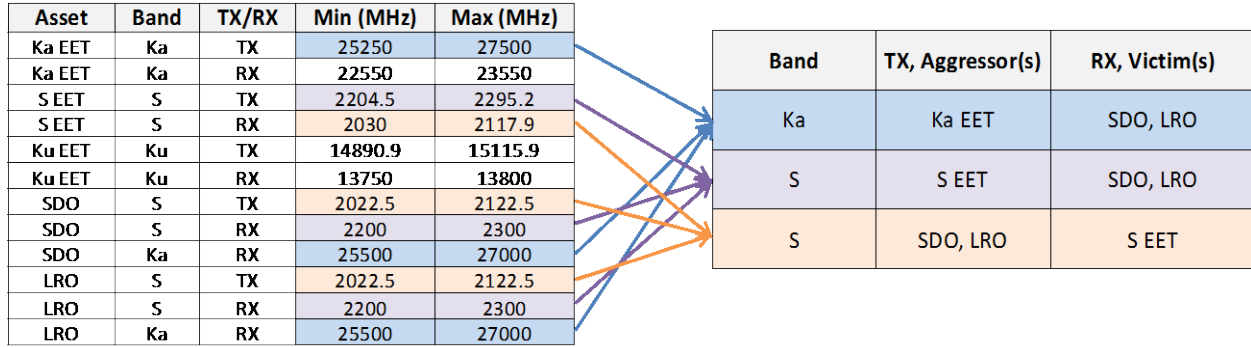


Figure 8: Reverse Banded Antennas at WSC

The S-band EET radiation necessary to test TDRS return services would possibly interfere with NEN S-band telemetry downlinks. The opposite problem also presented an issue; NEN S-band command uplinks had a chance to interfere with testing of TDRS forward services. Interference in either direction was not guaranteed and was influenced by the relative orientations of the aggressor and victim antennas, transmit-to-receive frequency separation, and the transmitted power from the aggressor antenna. A summary of the aggressors and victims and their operating frequency ranges are shown in Figure 8. In some cases S-band radiation from the EET was strong enough to saturate the modems connected to the NEN antennas. Any radiation from the NEN antennas in-band with the TDRS forward service under test prevented valid test artifacts from being gathered.

The Level 5 payload test campaign ran as a 24 hour/7 days a week campaign. However, the Level 5 test schedule proved dynamic and the payload test team moved from one frequency or service to another when they encountered issues in a given service. The test schedule uncertainty drove a daily mitigation process with the NEN users to minimize impacts to the payload test campaign while protecting the NEN user passes from interference.

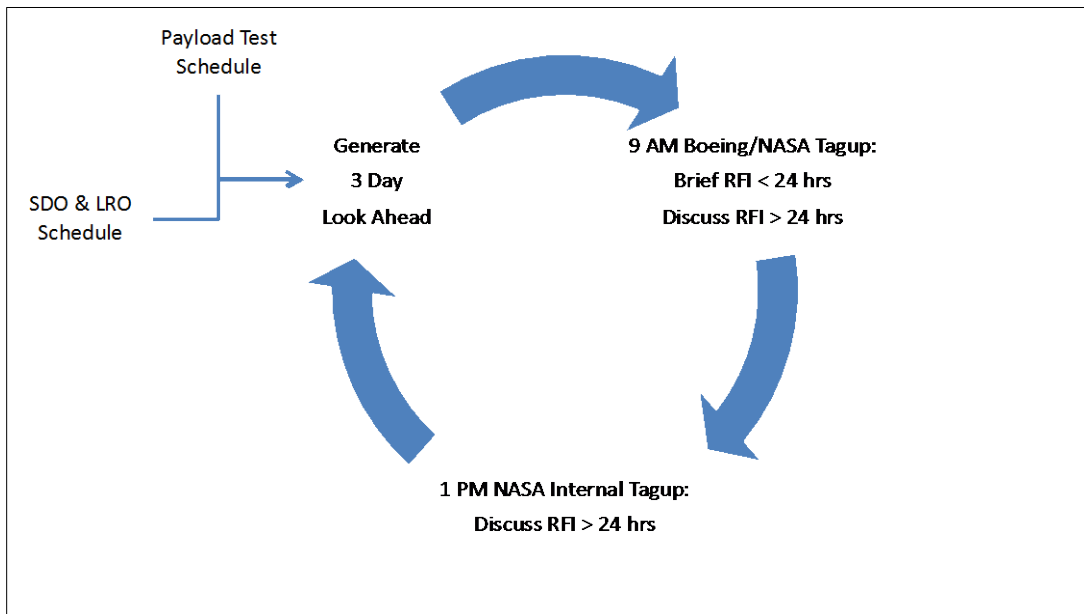


Figure 9: Daily RFI Coordination Process

This process evolved into a daily routine, shown in Figure 9, in which each day the Boeing test manager provided the NASA RFI coordinator an annotated test schedule. The coordinator generated a three-day look-ahead that enumerated TDRS tests and NEN user passes that had a high potential for interference. In cases where NEN user activity would impact TDRS testing, the Boeing test team was notified and the team moved testing or attempted to work through the individual event. TDRS testing that could interfere with a NEN user event was treated with higher

sensitivity, and tests that could not be moved had to stand down during the affected NEN events. The RFI team pursued other strategies, such as coordinating the payload test schedule to accommodate NEN user critical events scheduled well into the future (such as orbit maneuvers or instrument calibrations). For TDRS-K and L some NEN users that have a frequency allocation the same as the TDRS MA service were off-loaded from the NEN antennas. These users were moved to commercial NEN stations and the cost was absorbed by the TDRS project.

For TDRS-M, the RFI environment at WSC presented a greater challenge. The NEN antenna use had increased significantly since 2014, creating a higher potential for interference with TDRS testing. Also, local cell phone providers in the greater Las Cruces, NM region had deployed new 4G/LTE cells that operate in the Advanced Wireless Services (AWS)-1 band (2110 – 2155 MHz).² The AWS-1 cells interfered directly with testing of the MA Forward (MAF) service (2106.5 MHz) and the upper region of the S-band Single Access (SSA) forward service (TBD – 2117.5 MHz). This more challenging RFI environment resulted in three additional mitigations.

First, the TDRS project negotiated, and paid for, the complete unloading of the NEN antennas except for the LRO and SDO missions. Second, specific test procedures impacted by the AWS-1 cell interference were redlined to modify test frequencies. Third, the Goddard Space Flight Center (GSFC) Spectrum Manager negotiated with the AWS-1 cell providers for periods of cell downtime during which the test team gathered MAF test artifacts with clean spectrum. The TDRS project remains grateful to those providers for facilitating a successful TDRS-M payload test campaign.

The TDRS RFI mitigation process was developed primarily to protect the downlinks of the operational NEN users. Over three missions and seven calendar months of 24/7 testing, only one case of data loss for a NEN user was documented. Impacts to the Level 5 test campaign were minimal and the flexibility on both sides resulted in only hours of lost schedule for each satellite.

F. Doppler Anomaly

Eight users scheduled tracking services during the TDRS-K Level 6 period. Due to additional Level 5 spacecraft testing, Level 6 testing was performed in two segments, A and B in May and June, 2013. While all communication services provided through TDRS-K demonstrated full success, during the contacts with the Earth Observing System (EOS) missions, Terra, Aqua, and Aura, the 2-way Doppler data on SSA services exhibited large biases up to 0.5 Hz and strong drifts of 4.4×10^{-4} Hz/sec, uncharacteristic of the Doppler data from the TDRSS fleet overall. The data from TDRS-K violated the system specification on root mean squared phase noise of radiometric Doppler tracking 50 percent of the time using a point-by-point evaluation, with the 2-sigma point of the measured data set residing at 2.5 times the specification value of 0.032 Hz, rms.

The TDRS Project launched a root cause investigation, bringing in experts from relevant fields, following a fishbone layout of all potential error sources that contribute to the Doppler observation and computed Doppler used to form the “Observed-minus-Computed” residual (Figure 10). Besides the TDRS-K spacecraft, the leading candidates on the ground were the new TDRS-K modem unit, the SGLT chains involved in the Doppler observation, and the composite Cesium/Global Positioning System-referenced Common Time and Frequency System. Once ground subsystems and configurations were eliminated as the root cause, the investigation focused on the TDRS-K spacecraft. Additional user contacts with TDRS-K on a different SGLT in August 2013, in a period referred to as Level 6C, improved somewhat, but exhibited a bi-modal distribution with the number of specification violations exceeding those from the rest of the fleet. Figure 11 shows the anomalous Doppler performance on TDRS-K through a Cumulative Density Function against the operational TDRS fleet. With TDRS-L scheduled to launch in January 2014, it was imperative to determine whether the root cause lay with the TDRS-K spacecraft or to exonerate the relay prior to shipment of TDRS-L.

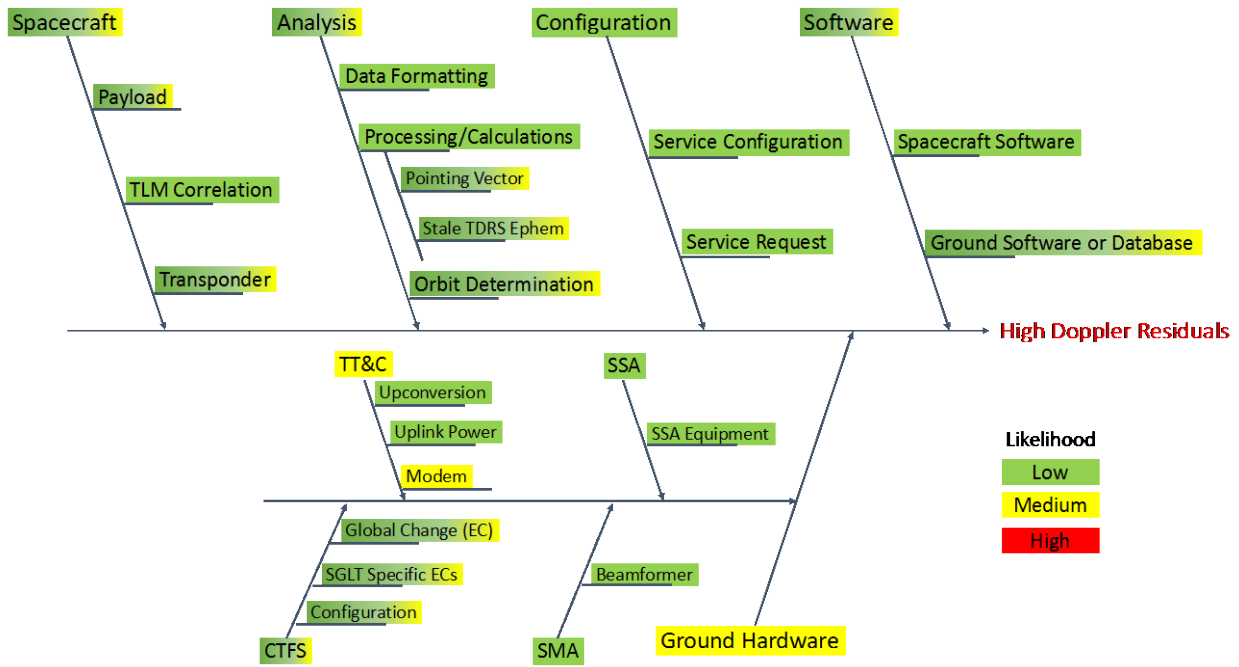


Figure 10. TDRS-K Doppler Anomaly Fishbone Potential Root Cause Summary

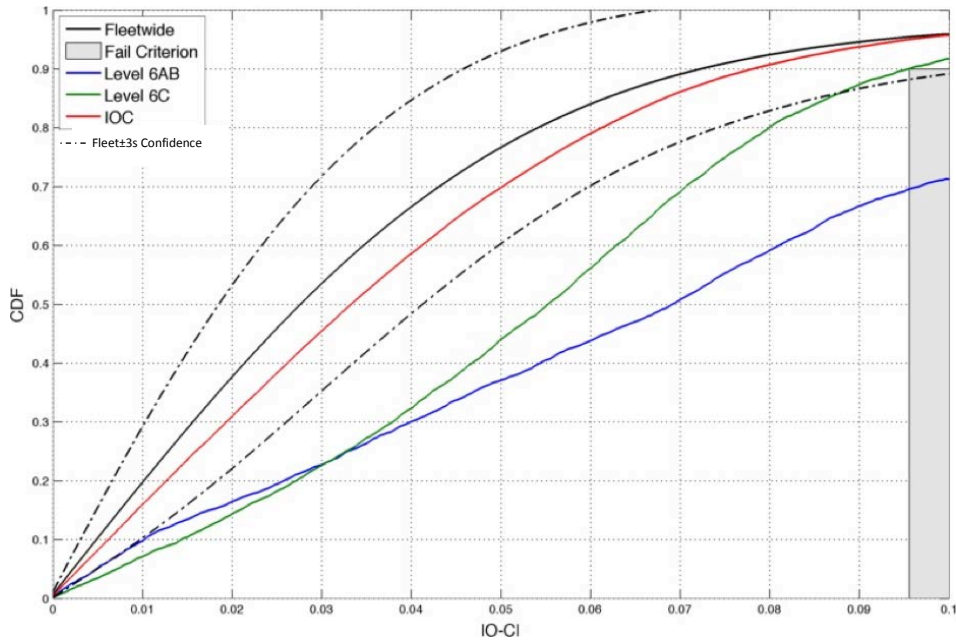


Figure 11. EOS Mission Cumulative Density Function for TDRS-K Test Periods vs Fleet

Orbit determination analysis for the EOS missions using the bi-modal Doppler data set in a highly-accurate sequential estimator, resulted in an error increase of 22% of the 20-meter (m) 3-sigma orbit knowledge requirement, mostly in the orbital cross-track component. Typical performance for the users in the sequential estimator based on the output covariance is 15 m during periods of low solar flux dynamics. A 22% error increase from poor Doppler data effectively depletes the necessary 5-m margin against the requirement for excursions introduced by solar flux-induced dynamics (e.g. during events such as solar storms, coronal mass ejections).

The investigation continued into the Interim Operations Capability (IOC) period with specific tests designed to bypass the link between the TDRS-K unique modem ground equipment and the TDRS-K relay spacecraft. The first day of test contacts continued to display the errant characteristics as noted in Level 6AB. However, starting on the second test day, the Doppler data from TDRS-K performed within specification, showed clean Gaussian distribution, and yielded results similar to the other TDRSS fleet members. Throughout the next month, Doppler data from test contacts continued to meet specification.

While the investigation obtained exonerating evidence for the leading candidate causes (including the spacecraft), the tests uncovered no conclusive evidence implicating any single candidate cause or sole contributing factor. All fishbone elements investigated showed in-spec performance in isolation. Much of the ground subsystems and the systems calculating the predicted Doppler and processing the Doppler residuals (observed minus predicted) proved exonerated through their common use in Doppler tracking data with the remainder of the fleet. Analysis and unit-level testing of the spacecraft reference frequency generation and distribution system identified a small contribution to the Doppler measurement noise from the spacecraft. The system relied on the same payload active units during all phases of Doppler performance measurement from the initial anomalous findings in Level 6AB, in the improved Level 6C period, to the IOC that ended with in-specification performance consistent with the fleet. Thus, given the unlikely nature for improved performance on-orbit from Level 6AB to IOC, the TDRS-K spacecraft was ruled out as a cause of the anomalous Doppler.

Following acceptance of TDRS-K, the TDRS project installed a Time Measurement Analysis System from the National Institute of Standards and Technology to monitor the performance of the SGLT time and frequency reference system through TDRS-M acceptance. TDRS-L and TDRS-M both exhibited within-specification Doppler performance on a total of 104 EOS contacts.

G. Aging Ground Segment

The aging ground segment at WSC presented many challenges to the successful commissioning of TDRS KLM. The STGT site was installed in the early 1990s and although rigorously maintained throughout the years, some components are beginning to fail. Prior to launch of TDRS-K, WSC underwent ground segment upgrades with a scope limited to providing the software and components needed to accommodate the operational differences between TDRS HIJ and TDRS KLM.

Integration of some of these components in the TT&C path introduced additional signal loss, resulting in unexpected RF measurements and occasional loss of signal lock. These additional losses presented the challenge of determining the source of the error, TDRS or ground system. The losses also created ambiguity in the range data, resulting in orbit determination difficulties. Implementation of shorter cables and line amplifiers mitigated the losses.

The challenge with the highest impact to testing and operations related to the RF infrastructure of the TT&C system. High Power Amplifier (HPA) and Antenna Control Unit (ACU) component failures caused the loss of TDRS uplink which resulted in autonomous TDRS reconfiguration requiring at least 45 minutes for recovery. The ACU-related failures included: polarizer alignment electronics, drive motor power supply, elevation control motor blower, drive logic control card chip, and emergency stop switch failures. Some of the events required transitioning TDRS to a different S-band TT&C resource while resolving the issue. One of the ACU-related failures resulted in TDRS residing on the S-band TT&C resource for nearly three weeks. The challenges presented by the RF infrastructure could only be mitigated through routine preventative maintenance which suffered from limitations. For example, the emergency stop (e-stop) switches reside near external access points on the antenna structure, exposed to the elements. The e-stop assembly consists of switch electronics mounted to the antenna structure in a sealed enclosure with an external plunger for the technicians to depress in case of emergency. As a sealed unit, the internal electronics cannot be inspected without breaking the seal and compromising the integrity of the enclosure.

The user services test equipment presented similar challenges. The S/Ku-band antenna system required frequent maintenance to provide adequate service. The HPAs used for signal generation required frequent rebuilding or replacement due to several different failure modes. The potentiometers and gears used to maintain pointing exhibited signs of excessive wear which resulted in the need to frequently halt testing and re-peak the antenna. Some of the symptoms of the pointing inaccuracies included rapid fluctuations of the noise floor and a large diurnal variation of signal level. To mitigate the known inaccuracy and instability of the antenna pointing, the schedule, as well as some key portions of individual tests, incorporated antenna peaking functions.

OOT verification of the MA system relied on an HIJ era test set. The HIJ program delivered two identical racks which were maintained between HIJ OOT and TDRS-K launch. To complete TDRS-K and L OOT, components from the backup rack were harvested to replace failed units in the primary leaving TDRS-M with one aged rack without redundancy. GSFC engineers designed, built, tested, and delivered a replacement unit for backup which is discussed in greater detail in Section H.

H. Multiple Access Forward Antenna Calibration Equipment

TDRS KLM payload on-orbit test program includes procedures to calibrate the MAF phased array on the spacecraft. The MAF array calibration procedure requires custom test equipment at the ground station that processes the received MAF carrier to generate estimates of phase and amplitude error for each individual MAF array element. The manufacturer’s payload systems engineering team uses the estimates of phase and amplitude error to upload new phase and amplitude coefficients to the MAF on-board beamformer to optimize the transmit array’s gain.

The previous TDRS program (HIJ) produced two multiple access array calibration units, referred to as the MA Autocal. The MA Autocal is capable of calibrating both the MAF and MAR arrays on the 2nd generation spacecraft. In 2013, during TDRS-K POOT, 1 of 2 MA Autocal units failed and was unable to be repaired due to parts obsolescence. In 2014, TDRS-L POOT was successful using the 2nd MA Autocal unit, but resulted in a risk written against TDRS-M POOT because of the three year separation between TDRS-L and the planned August 2017 launch of TDRS-M.

During TDRS-L IOC testing, a proof of concept system for a MA Autocal replacement based on a software defined radio (SDR) device demonstrated successful performance and the TDRS project decided to develop the Multiple Access Replacement Calibrator (MARC) as a contingency for TDRS-M POOT. The MARC is based on the Universal Software Radio Peripheral (USRP), a software radio device popular in the SDR community. Figure 12 maps the MARC hardware to functionality.

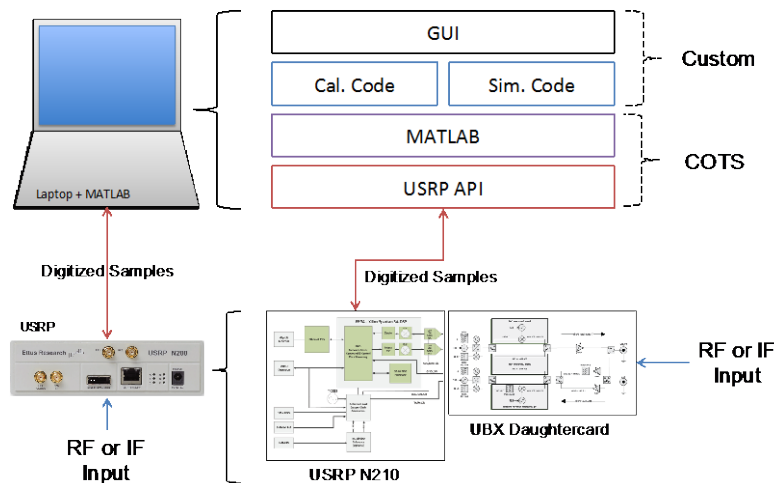


Figure 12: MARC Architecture

The MARC utilizes a USRP version N210 with a UBX daughter card. The USRP performs frequency up/down conversion, filtering, amplification, and sampling to transfer the microwave input into a digitized signal. The UBX daughter card provides a tuneable range from 10 MHz to 6 GHz, inclusive of both the Intermediate Frequency (IF) (370 MHz) and RF (2016.4 MHz) test ports used at WSC. The USRP is used to sample the MAF carrier at a 200 kbps rate during the calibration sequence, and the resulting digitized signal is saved to the MARC laptop hard drive. MATLAB, which includes a USRP API plugin, is used to configure the USRP, start signal recording, and then process the recorded signal to generate array calibration estimates and to generate a report similar to the legacy calibrator. Although all the calibration steps could be accomplished via the MATLAB command line, a GUI was developed to ease use by operators at WSC. The GUI allows the user to configure the test set-up and enable and disable features in the MATLAB code. GSFC civil servants developed the MARC GUI, calibration code, and simulation code (test benches).

To perform a calibration of the MAR or MAF arrays, the phases of all elements for a given beam are initialized for pointing at a fixed ground station. These settings constitute the 0 degree setting. To calibrate a single antenna element, the phase of that element is sequenced through the phase states corresponding to 180, 90, and 270 relative to the reference state. Each one of these cycles is preceded by a sync pulse. The MARC MATLAB code finds the sync pulses, performs the power measurements, and calculates the element phase and amplitude errors from the power measurements at the four phase states. This procedure is repeated for each element in the array.

Prior to TDRS-M launch, MARC testing involved three phases; (1) software testing that stressed the MATLAB calibration code, (2) bench testing that demonstrated GUI operation, connectivity to the USRP, and verified calibration with a simulated IF/RF input, and (3) live-sky testing with an operational satellite and the MA Autocal in order to perform side-by-side comparisons of MARC calibration results with the legacy MA Autocal.

Given that the final verification testing execution occurred on an operational TDRS, changing the MAF configuration on-board the satellite posed too great a risk. With this in mind, the verification testing did not close the loop with the spacecraft, i.e. the calibration results were not used to adjust the MAF calibration on the spacecraft. An initial test was executed in December of 2016 while the run-for-record was executed in February 2017. The STGT East EET and TDRS-12 were used for both tests. The MA Autocal was connected to the EET IF port for all tests, while the MARC was connected to either the IF port or the RF port (with a 3 dB splitter) depending on the test configuration. The MARC testing pass/fail criteria included reproducing the MA Autocal report and calculating phase errors within 50% of the commandable phase adjustment in the MA beamforming ASICs.

Both MARC tests successfully demonstrated that the MARC performance met all pass/fail criteria. After the final test, WSC received the hardware, configuration managed software, as well as associated documentation including a user's manual and verification test report. A second unit remained in storage at GSFC. During the execution by Boeing of TDRS-M POOT in the fall of 2017, the legacy MA Autocal did not fail and therefore, the MARC was not used for the MAF calibration. However, the system remains at WSC as a backup to the legacy system and as a tool for recording raw digitized IF/RF data should any future payload debugging be required.

V. Future Architecture

The Space Network architecture was conceived in the 1970s and started operations in the 1980s. The advancement in technology and unique capabilities offered by TDRS has maintained the network's relevance through the Space Shuttle program, Earth Observation Spacecraft fleet, International Space Station, and the Evolved Expendable Launch Vehicle program, through today. However, NASA foresees the next decade as one of transition. Optical communications and navigation technology offers the agency an opportunity to harness a new technology S-curve to meet the needs of new science and exploration missions. NASA will also deliver communication and navigation services in an autonomous, on-demand fashion to reduce or eliminate up-front scheduling of services.

The first step in this transition will be refreshing Space Network to meet the needs of current and committed users through the 2020s. The TDRS KLM program refreshed the space segment of the Space Network, while the SGSS project will refresh the entire SN ground system. While refreshing the SN NASA is developing and deploying laser communications and navigation systems operationally through demonstration missions and key pathfinder missions. These early demonstrations will allow the next generation requirements and architecture to be refined within the next 5 years and deployed in the mid to late 2020s.

A. Space Network Ground Segment Sustainment

The 1990s era SN ground segment is beyond its planned lifetime and is being replaced by the SGSS project. SGSS's goal is to replace all ground segment hardware except for the 18 meter space-to-ground antennas that service each TDRS satellite.³ The SGSS architecture will shrink the ground segment's equipment footprint by a factor of 10 by employing commodity server farms hosting virtual machines. SGSS will replace the current ground architecture's analog RF and IF signal distribution with a 10 Gb Ethernet digital IF bearer plane connected to a digital modem pool. The new SGSS modems will support low density parity check codes at rates up to 1.2 Gbps for Ka-band services. SGSS's modern architecture will provide a means to expand and upgrade SN services while addressing reliability of the aged ground equipment currently in service.

B. The Transition to Optical Communications

TDRS-M, the 13th Tracking and Data Relay Satellite, is likely the last of its kind. NASA is investing heavily to mature optical communications technology by flying technology demonstration missions to achieve this goal. Two such missions are the Lunar Laser Communications Demonstration that launched in 2013 and the Laser Communications Relay Demonstration expected to launch in 2019. These initial investments in optical technology will allow for operational infusion into optical Earth relays, near-Earth ground terminals, deep space ground terminals, and user terminals. Optical communications promises data rates up to 100 Gbps for LEO missions direct to the Earth.⁴ Coherent optical communications will allow for optometric ranging to accuracies of 10s of nanometers, a 4-5 order of magnitude improvement over current microwave techniques.⁵ An Earth-relay architecture that includes 100 Gbps optical crosslinks will eliminate the need for relay ground stations outside the continental United States. The user services benefits coupled with a smaller terminal envelope provide a clear impetus to deploy optical communications

technology. NASA's transition from exclusively microwave based communications to a mix of optical communications is targeted to occur over the next decade.

The Space Network currently supports 40 robotic and human missions and continues to expand its customer base. As the older TDRS retire from service, continued microwave relay capacity is required to service these missions already in operations. Planning for an Earth relay spacecraft as the successor to the TDRS program has already started, with relevant RFIs released by NASA in 2017 and 2018. NASA is open to new ways to deliver backwards compatible microwave relay capacity; a fractionated relay that only provides a subset of the services found on a current TDRS, hybrid optical/microwave relays, or partnering with commercial satellite communication providers to deliver the services required by operational customers. The next decade will be exciting to witness as NASA transitions from the 1980s era Space Network architecture to an optical based architecture able to meet the demands of new NASA missions.

C. Next Generation Architecture Services

TDRS-M represents the last chapter of the current TDRS constellation, and NASA is already looking forward to the communication and tracking needs of the future, re-imagining the architecture of the network itself. The Earth Regimes Network Evolution Study (ERNESt) proposed the development of a near-Earth communication network consisting of a new generation of ground and space-based communication assets. This network would abandon the current network architecture defined by the Apollo era Manned Space Flight Network and Space Shuttle era SN, and transition to the architectural concepts that enable today's terrestrial wireless networks. ERNESt's Space Mobile Network (SMN) will provide a user experience that emulates some services provided by modern smart phones, particularly the automated delivery of communication services and always available navigation and timing capability.

This move from a centrally managed, fully scheduled, deterministic network topology to a user-initiated, decentralized, delay-tolerant, non-deterministic network topology requires a shift to one-way, non-coherent observations and autonomous onboard navigation. And this introduces several challenges. Production of one-way observations useful for orbit determination is predicated on precise synchronization of the transmitter and receiver to a common timescale, and stable frequency reference. Additionally, signal acquisition becomes a fundamental constraint to autonomous network scheduling - if the network does not have accurate predictive ephemerides for the users, then it cannot acquire their signals, nor can it autonomously and reliably schedule network resources to meet user demand access requests. Autonomous, onboard navigation becomes essential.

Both of these challenges are addressed by the Next Generation Broadcast Service (NGBS) concept. Through NGBS, TDRS spacecraft and network ground assets transmit distinguishable signals and data to enhance user operations and enable autonomous onboard navigation via a broadcast beacon service. The baseline beacon design provides coverage of the Earth and LEO from a geosynchronous relay, produced through a particular configuration of four MAF elements.⁶ The transmitted message provides space environment data (e.g., ionosphere, Kp index for drag), Earth Orientation Parameters, relay ephemerides and maneuver windows, global Differential GPS corrections, and GPS integrity data. Message fields are also provided for unscheduled, on-demand user commanding. The beacon signal includes a PN ranging code synchronized with a global common time and frequency reference for time transfer, one-way forward Doppler and pseudo-ranging. The navigation features of NGBS are capable of supporting standalone navigation in LEO with three beacons.⁷

Providing some means of user navigation is essential for many components of the future network vision, including User Initiated Services (UIS). UIS is a network access method that enables responsiveness to unplanned events. New mission concepts are possible when platforms can switch operations to support event-based or transient phenomena, such as gamma ray bursts and gravitational waves, and participate in ad-hoc, multi-observatory collaborations. An initial UIS on-orbit experiment was performed with the SCaN Test Bed on the International Space Station in late 2017⁸, and a UIS demo on the SMN User Demonstration Satellite is planned in the near future.⁹ The close interdependence of communication and navigation will be just as important in the era of optical communications, and systems are being developed that support highly precise range and range rate optometrics.⁴

Conclusion

Acceptance of the TDRS-M spacecraft in early 2018, marks the completion of a constellation of communication and navigation satellites that began service in the early 1980s. Lessons learned from the launch and orbit raising and on orbit testing of the TDRS-K and L spacecraft were carried forward and applied during the successful 2017 TDRS-M campaign. The lessons learned during TDRS KLM are also applicable to upcoming ground segment updates and future NASA missions with similar components or operations concepts, providing continuity of communication and navigation services to the user community.

VI. Acknowledgments

The authors of this paper would like to thank everyone involved in the successful orbit raising, on orbit testing, and acceptance of the 3rd generation TDRS spacecraft including The Boeing Company personnel, members of the TDRS project at NASA Goddard Space Flight Center, and the Space Communications and Network Services contract Spacecraft Operations Engineering and Space Network teams at NASA's White Sands Complex.

VII. References

- ¹K. McCarthy, F. Stocklin, B. Geldzahler, D. Friedman, P. Celeste, "NASA's Evolution to Ka-Band Space Communications for Near-Earth Spacecraft," SpaceOps 2010, Huntsville, AL, April 25-30, 2010.
- ²FCC Auction of Advanced Wireless Services, Public Notice DA 06-1882, September 9, 2006.
- ³Gitlin, T. and Walyus, K., "NASA's Space Network Ground Segment Sustainment Project Preparing for the Future," Proceedings of The 12th International Conference on Space Operations, 11-15 Jun. 2012, Stockholm, Sweden
- ⁴G. Yang, W. Lu, M. Krainak and X. Sun, "High-precision ranging and range-rate measurements over free-space-laser communication link," 2016 IEEE Aerospace Conference, Big Sky, MT, 2016, pp. 1-13. doi: 10.1109/AERO.2016.7500652
- ⁵D. J. Israel, G. W. Heckler and R. J. Menrad, "Space Mobile Network: A near Earth communications and navigation architecture," 2016 IEEE Aerospace Conference, Big Sky, MT, 2016, pp. 1-7. doi: 10.1109/AERO.2016.7500669
- ⁶G. Heckler, C. Gramling, J. Valdez, and P. Baldwin, "TDRSS Augmentation Service for Satellites," SpaceOps 2016, Daejeon, Republic of Korea, May 2016.
- ⁷J. Valdez, B. Ashman, C. Gramling, G. Heckler, and R. Carpenter, "Navigation Architecture for a Space Mobile Network", 39th American Astronautical Society Guidance and Control Conference, Breckenridge, CO, February 2016.
- ⁸D. Mortensen, C. Roberts, R. Reinhart, and D. Chelmins, "Automated Spacecraft Communications Service Demonstration Using NASA's SCaN Testbed", SpaceOps 2018, Marseilles, France, May-June 2018.
- ⁹H. Shaw, J. King, D. Israel, and C. Roberts, "Space Mobile Network User Demonstration Satellite (SUDS) for a practical on-orbit demonstration of User Initiated Services", SpaceOps 2018, Marseilles, France, May-June 2018.
- ¹⁰Figure 5: TDRS L Flight Operations Review, Section 5.3.1A Operations: Attitude Control Subsystem/Dynamics, Eric Roth, Boeing, November 8, 2013
- ¹¹Figure 6 & 7: TDRS-M Deployment Attitude Change, Yaw Limit Cycle ERB Data Package, Eric Roth, Boeing, April 30, 2014